

How orbital angular momentum affects beam shifts in optical reflection

M. Merano, N. Hermosa, and J. P. Woerdman

*Huygens Laboratory, Leiden University,
P.O. Box 9504, 2300 RA Leiden, The Netherlands*

A. Aiello

*Max Planck Institute for the Science of Light,
Günter-Scharowsky-Straße 1/Bau 24, 91058 Erlangen, Germany*

Abstract

It is well known that reflection of a Gaussian light beam (TEM_{00}) by a planar dielectric interface leads to four beam shifts when compared to the geometrical-optics prediction. These are the spatial Goos-Hänchen (GH) shift, the angular GH shift, the spatial Imbert-Fedorov (IF) shift and the angular IF shift. We report here, theoretically and experimentally, that endowing the beam with Orbital Angular Momentum (OAM) leads to coupling of these four shifts; this is described by a 4×4 mixing matrix.

PACS numbers: 42.79.-e, 41.20.Jb, 42.25.Gy, 78.20.-e

Introduction. — The reflection of a light beam by a mirror shows subtle aspects that were first conjectured by Newton [1]: the center of the reflected beam may show a small spatial shift *in* the plane of incidence, relative to the position predicted by geometrical optics. This shift has been named after Goos and Hänchen (GH) who were the first to observe it in total internal reflection (TIR) [2]. In more recent years the GH shift has been studied in a large diversity of cases, ranging from photonic crystals [3] to neutron optics [4]. Additionally, there is a spatial shift *perpendicular* to the plane of incidence, the so-called Imbert-Fedorov shift (IF) [5, 6]. There exist also *angular* GH and IF shifts, both of which have been demonstrated recently in external reflection [7, 8]. The angular shifts can be seen as shifts in wave-vector space [8–10]; we note that the angular IF shift is also known as the Spin Hall Effect of Light (SHEL) [8]. All shifts depend on the polarization, i.e. on the Spin Angular Momentum of the incident photons.

We are interested in the question how these beam shifts are affected when the light beam is endowed with Orbital Angular Momentum (OAM). OAM is a relatively novel degree of freedom of a light beam that has found applications from optical tweezers to quantum information science [11, 12]. Theoretically, a treatment of the effect of OAM on beam shifts has already been given, first by Fedosoyev [13] and then by Bliokh *et al.* [14]. However, these treatments were based on the concept of conservation of angular momentum. Here we prefer a more direct approach based on straightforward application of Snell’s law and the Fresnel equations since in principle the use of angular momentum conservation laws is fraught with difficulties [15]. (However, our theoretical results will turn out to be fully consistent with the earlier work [13, 14]). Experimentally, Okuda and Sasada have studied the deformation of an OAM carrying beam by TIR very close to the critical angle [16]; however, they did not report GH and IF shifts. Dasgupta and Gupta have measured the IF shift of an OAM beam reflected by a dielectric interface, but only for the spatial case [17].

It is the purpose of this Letter to report a theoretical and experimental study of the effect of OAM on the four basic shifts: spatial GH, angular GH, spatial IF and angular IF. We find that these shifts are coupled by OAM; this is described by an OAM dependent 4×4 mixing matrix. We have experimentally confirmed this mixed occurrence of GH and IF shifts.

Theory. — Consider a monochromatic beam containing a continuous distribution of wave-vectors \mathbf{k} centered around $\mathbf{k}_0 = k_0 \hat{\mathbf{z}}_i$, where $\hat{\mathbf{z}}_i$ is a unit vector along the central propagation direction of the incident beam: $\mathbf{k} = k_0 \hat{\mathbf{k}} = \mathbf{k}_0 + \mathbf{q}$, with $\mathbf{q} = \mathbf{q}_T + q_L \hat{\mathbf{z}}_i$ and $\mathbf{q}_T \cdot \hat{\mathbf{z}}_i = 0$.

Using the notation of Fig. 1, we write $q_T/k_0 = \sin \alpha$ and $q_L/k_0 = 1 - \cos \alpha$ with $q_T = |\mathbf{q}_T|$ and $\alpha = \arccos(\hat{\mathbf{k}} \cdot \hat{\mathbf{k}}_0)$. A collimated beam has a narrow distribution of wave-vectors around \mathbf{k}_0 such that $\sin \alpha \cong \alpha \ll 1$ with $q_T/k_0 \cong \alpha \ll 1$ and $q_L/k_0 \cong (q_T/k_0)^2/2$. Thus, if we write $\mathbf{q} = k_0(\hat{\mathbf{x}}_i U + \hat{\mathbf{y}} V + \hat{\mathbf{z}}_i W)$ with $W = \sqrt{1 - U^2 - V^2}$, we can assume $U, V \ll 1$ without significant error.

Let $\mathbf{E}^I(\mathbf{r}t)$ be the electric field of the incident beam. Upon reflection this field evolves to $\mathbf{E}^R(\mathbf{r}t)$ which is to be found. From the linearity of the wave equation it follows that $\mathbf{E}^R(\mathbf{r}t)$ can be determined by studying the action of the interface upon each plane wave field $\mathbf{A}^I(\mathbf{k}) = \mathbf{f}_\perp(\mathbf{k}) \exp(i\mathbf{k} \cdot \mathbf{r} - i\omega t)$ that constitutes $\mathbf{E}^I(\mathbf{r}t)$, with $\omega = |\mathbf{k}|c$. According to Refs. [18, 19], we assume the polarization dependent amplitude of $\mathbf{A}^I(\mathbf{k})$ equal to $\mathbf{f}_\perp(\mathbf{k}) = \hat{\mathbf{f}} - \hat{\mathbf{k}}(\hat{\mathbf{k}} \cdot \hat{\mathbf{f}}) \equiv a_p(\mathbf{k})\hat{\mathbf{x}}_k + a_s(\mathbf{k})\hat{\mathbf{y}}_k$ where $\hat{\mathbf{f}} = f_p\hat{\mathbf{x}}_i + f_s\hat{\mathbf{y}}$ is a \mathbf{k} -independent complex unit vector that fixes the polarization of the incident beam, and $\hat{\mathbf{y}}_v = \hat{\mathbf{z}} \times \mathbf{v}/|\hat{\mathbf{z}} \times \mathbf{v}|$, $\hat{\mathbf{x}}_v = \hat{\mathbf{y}}_v \times \mathbf{v}$ denote a pair of mutually orthogonal real unit vectors that together with $\hat{\mathbf{v}} = \mathbf{v}/|\mathbf{v}|$ form a right-handed Cartesian reference frame $K_v = \{\hat{\mathbf{x}}_v, \hat{\mathbf{y}}_v, \hat{\mathbf{v}}\}$ attached to \mathbf{v} .

When the beam is reflected at the interface, each plane wave evolves as: $\mathbf{A}^I(\mathbf{k}) \rightarrow \mathbf{A}^R(\mathbf{k})$ where

$$\mathbf{A}^R(\mathbf{k}) = [r_p(\theta_k) a_p(\mathbf{k}) \hat{\mathbf{x}}_{\tilde{\mathbf{k}}} + r_s(\theta_k) a_s(\mathbf{k}) \hat{\mathbf{y}}_{\tilde{\mathbf{k}}}] \chi(\tilde{\mathbf{r}}t), \quad (1)$$

and $\chi(\tilde{\mathbf{r}}t) = \exp(i\tilde{\mathbf{k}} \cdot \mathbf{r} - i\omega t) = \exp(i\mathbf{k} \cdot \tilde{\mathbf{r}} - i\omega t)$. The notation $\tilde{\mathbf{v}}$ indicates the mirror image of the vector \mathbf{v} with respect to the interface: $\tilde{\mathbf{v}} = \mathbf{v} - 2\hat{\mathbf{z}}(\hat{\mathbf{z}} \cdot \mathbf{v})$, with $\tilde{\mathbf{v}} \cdot \mathbf{u} = \mathbf{v} \cdot \tilde{\mathbf{u}}$ [20]. Moreover, $r_p(\theta_k)$ and $r_s(\theta_k)$ are the Fresnel reflection coefficients at incidence angle $\theta_k = \arccos(\hat{\mathbf{k}} \cdot \hat{\mathbf{z}})$ for p and s waves, respectively. By direct calculation it is not difficult to

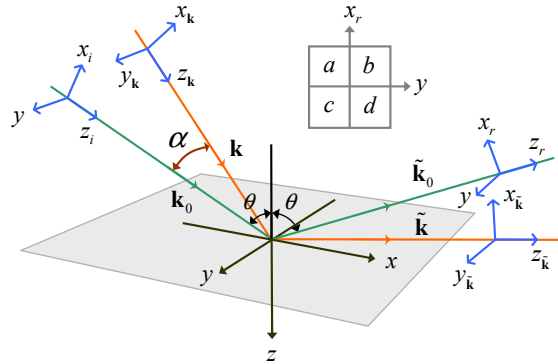


FIG. 1: (Color online) Geometry of beam reflection at a dielectric interface. Inset shows quadrant detector with sensitive areas a, b, c, d .

show that, up to first order in U, V , $\mathbf{A}^R(\mathbf{k}) \simeq \hat{\mathbf{x}}_r A_p^R + \hat{\mathbf{y}} A_s^R$ with

$$A_\lambda^R(\mathbf{k}) \simeq f_\lambda r_\lambda \chi(-X + X_\lambda, Y - Y_\lambda, Z, t), \quad (2)$$

where $\lambda \in \{p, s\}$, $r_\lambda = r_\lambda(\theta)$ ($\theta \equiv \theta_{\mathbf{k}_0}$) and

$$X_p = -i \frac{\partial \ln r_p}{\partial \theta}, \quad Y_p = i \frac{f_s}{f_p} \left(1 + \frac{r_s}{r_p} \right) \cot \theta, \quad (3)$$

with $X_s = X_p|_{p \leftrightarrow s}$ and $Y_s = -Y_p|_{p \leftrightarrow s}$. The limit of total reflection is achieved by letting $r_p \rightarrow 1$ and $r_s \rightarrow -1$ where Eq. (3) reduces to $X_p = 0 = X_s$ and $Y_p = 0 = Y_s$. Moreover, we have introduced the dimensionless coordinates $X = k_0 x_r$, $Y = k_0 y$, and $Z = k_0 z_r$, where z_r is the distance from the waist of the incident beam to the detector measured along the trajectory of the beam.

The passage from the single plane wave field $\mathbf{A}^R(\mathbf{k})$ to the total electric field $\mathbf{E}^R(\mathbf{r}t)$ is realized by substituting the plane wave scalar amplitude $\chi(\mathbf{r}t)$ into Eq. (2), with the electric field scalar amplitude $E(\mathbf{r}t)$ describing the spatial distribution of the incident beam. In the present case, as we want to study the behavior under reflection of OAM beams, we choose $E(\mathbf{r}t) = \psi_\ell(\mathbf{r}) \exp(-i\omega t)$, being $\psi_\ell(\mathbf{r})$ the Laguerre-Gauss paraxial field with OAM index $\ell \in \{0, \pm 1, \pm 2, \dots\}$ and radial index $p = 0$: $\psi_\ell(X, Y, Z) \propto \exp[-(X^2 + Y^2)/(2\Lambda + i2Z)] (X + is_\ell Y)^{|\ell|}$, with $s_\ell = \text{sign}(\ell)$ and $\Lambda = k_0(k_0 w_0^2/2)$ denoting the dimensionless Rayleigh range of the beam with waist w_0 [21]. Thus, the transverse electric field of a Laguerre-Gauss beam reflected by a plane interface can be written as:

$$E_\lambda^R(\mathbf{r}t) \simeq f_\lambda r_\lambda \psi_\ell(-X + X_\lambda, Y - Y_\lambda, Z) \exp(-i\omega t). \quad (4)$$

In this expression the terms X_λ and Y_λ are responsible for the GH [10] and IF [14] shifts of the center of the beam, respectively. These displacements can be assessed by measuring the position of the center of the reflected beam with a quadrant detector centered at $x_r = 0$, $y = 0$ along the reference axis z_r attached to the reflected central wave vector $\tilde{\mathbf{k}}_0 = k_0 \hat{\mathbf{z}}_r$. A quadrant detector has four sensitive areas, denoted with a, b, c, d in the inset of Fig. 1, each delivering a photocurrent I_a, I_b, I_c, I_d respectively, when illuminated. The two currents $I_x = (I_a + I_b) - (I_c + I_d)$ and $I_y = (I_b + I_d) - (I_a + I_c)$ are thus proportional to the x - and the y -displacement of the beam intensity distribution relative to the center of the detector, respectively.

If $\ell = 0$, $\psi_0(-X + X_\lambda, Y - Y_\lambda)$ reduces to a shifted fundamental Gaussian beam, and in the hypothesis of small deviations $X_\lambda, Y_\lambda \ll 1$, a straightforward calculation furnishes

$$\frac{I_x}{I} = N_0 \left(\Delta_{\text{GH}} + \frac{Z}{\Lambda} \Theta_{\text{GH}} \right), \quad \frac{I_y}{I} = N_0 \left(\Delta_{\text{IF}} + \frac{Z}{\Lambda} \Theta_{\text{IF}} \right), \quad (5)$$

where $I = I_a + I_b + I_c + I_d$, and $N_0 = \sqrt{2/(\pi\sigma^2)}$ with $\sigma^2 = (\Lambda/2)\sqrt{1 + Z^2/\Lambda^2}$. Here we have defined the two spatial (Δ) and the two angular (Θ) shifts $\Delta_{\text{GH}} = \sum_\lambda w_\lambda \text{Re}(X_\lambda)$, $\Delta_{\text{IF}} = \sum_\lambda w_\lambda \text{Re}(Y_\lambda)$ and $\Theta_{\text{GH}} = \sum_\lambda w_\lambda \text{Im}(X_\lambda)$, $\Theta_{\text{IF}} = \sum_\lambda w_\lambda \text{Im}(Y_\lambda)$, respectively, with $w_\lambda = |r_\lambda f_\lambda|^2 / (|r_p f_p|^2 + |r_s f_s|^2)$.

If $\ell \neq 0$, Eq. (5) becomes

$$\frac{I_x}{I} = N_\ell \left(\Delta_{\text{GH}}^\ell + \frac{Z}{\Lambda} \Theta_{\text{GH}}^\ell \right), \quad \frac{I_y}{I} = N_\ell \left(\Delta_{\text{IF}}^\ell + \frac{Z}{\Lambda} \Theta_{\text{IF}}^\ell \right), \quad (6)$$

where $N_\ell = N_0 \Gamma(|\ell| + 1/2) / [\Gamma(|\ell| + 1) \sqrt{\pi}]$ ($\Gamma(x)$ denotes the Gamma function), and

$$\begin{bmatrix} \Delta_{\text{GH}}^\ell \\ \Theta_{\text{IF}}^\ell \\ \Delta_{\text{IF}}^\ell \\ \Theta_{\text{GH}}^\ell \end{bmatrix} = \begin{bmatrix} 1 & -2\ell & 0 & 0 \\ 0 & 1 + |2\ell| & 0 & 0 \\ 0 & 0 & 1 & 2\ell \\ 0 & 0 & 0 & 1 + |2\ell| \end{bmatrix} \begin{bmatrix} \Delta_{\text{GH}} \\ \Theta_{\text{IF}} \\ \Delta_{\text{IF}} \\ \Theta_{\text{GH}} \end{bmatrix}. \quad (7)$$

Equation (7) clearly displays the mixing between spatial and angular GH and IF shift, occurring only for $\ell \neq 0$, and it is in agreement with the results presented in Ref. [14], apart from the factor “2” in front of ℓ [22]. Notice that the polarization dependence of the four ℓ -dependent shifts on the left side of Eq. (7) resides in the four ℓ -independent shifts on the right side of the same equation. It turns out that the 4×4 mixing matrix itself is polarization-independent. It should be noticed that in TIR, since the Fresnel coefficients are purely imaginary, both GH and IF angular shifts Θ_{GH} and Θ_{IF} are identically zero [23]. Thus, in this case, from Eq. (7) it follows that mixing vanishes.

Experimental set-up. — Our experimental set-up is shown in Fig. 2. A home built HeNe laser ($\lambda_0 = 633 \text{ nm}$) is forced to operate in a single higher-order Hermite-Gaussian (HG_{nm}) mode with $m = 0$ by insertion of a $40\text{-}\mu\text{m}$ diameter wire normal to the axis of the laser cavity [24]. The HG_{n0} beam is sent through an astigmatic mode converter consisting of two cylinder lenses, with their common axis oriented at 45° relative to the intra-cavity wire. This introduces a Gouy phase which converts the HG_{n0} beam in a $\text{LG}_{\ell p}$ beam with $\ell = n$ and $p = 0$ [24]. Lenses 1 and 2 are used for mode matching; the beam leaving lens 2 is collimated

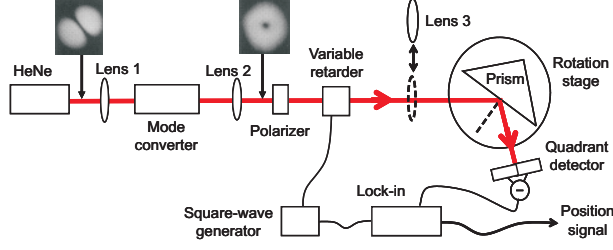


FIG. 2: (Color online) Experimental set-up. The insets show the HG_{10} and LG_{10} mode profiles. The quadrant detector measures the OAM controlled shift of the reflected beam in the plane of incidence (GH shift) and perpendicular to it (IF shift). Both the GH and the IF shift have a spatial and an angular contribution. See text for further details.

with a waist parameter $w_0 = 775 \mu\text{m}$, a power of typically $600 \mu\text{W}$ and a polarization set by a linear polarizer. We have incorporated the option to greatly enhance the angular spread of the beam by inserting lens 3 ($f = 70 \text{ mm}$), leading to $w_0 = 19 \mu\text{m}$. Either with or without lens 3 present, the beam is externally reflected by the base plane of a glass prism (BK7, $n = 1.51$). We measured the polarization-differential shifts of the reflected $LG_{\ell 0}$ beam with a calibrated quadrant detector. We also obtained these shifts for the fundamental LG_{00} beam ($= \text{TEM}_{00}$) by simply removing the intra-cavity wire from the HeNe laser.

It follows from Eqs. (5-6) that using a collimated incident beam, i.e. $\Lambda \gg Z$, leads to total predominance of the spatial shift. On the other hand, the use of a focused beam, i.e. $\Lambda \ll Z$, leads to total predominance of the angular shift. These two extreme cases were realized in our experiment by removal respectively insertion of lens 3. Specifically, the value of the Rayleigh range $L = k_0 w_0^2 / 2$ was 2.96 m and 1.8 mm , respectively; as standard we have chosen the distance z_r between the beam waist and the quadrant detector to be 9.5 cm . We experimentally checked the angular nature of the shift (where expected) by verifying that the detector signal depended linearly on changes in z_r .

We performed all measurements by periodically (2.5 Hz) switching the polarization of the incident beam with a liquid-crystal variable retarder and by synchronously measuring (with a lock-in amplifier) the relative beam position for one polarization with respect to the other [7, 25]. Experimentally we were restricted to using the first-order LG modes ($\ell = \pm 1$) by the low gain of the HeNe laser.

Experimental results and comparison with theory.— Our experimental results for the

polarization-differential shifts versus the angle of incidence are reported in Fig. 3, together with the theoretical curves ($\ell = 0$ and $\ell = \pm 1$) which are based upon Eqs. (5-6). The four

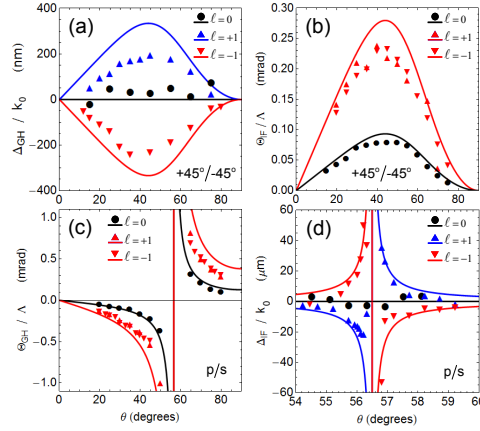


FIG. 3: (Color online) Reflective beam shift for partial dielectric reflection from an air-glass interface as a function of the angle of incidence. Plotted curves are the theoretical polarization-differential shifts for the two polarizations indicated in each panel. Experimental data and theoretical curves refer to $\ell = 0$ and $\ell = \pm 1$. The panels display the spatial GH shift (a), angular IF shift (b), angular GH shift (c) and spatial IF shift (d). Here $k_0 = 2\pi/\lambda_0$; see text for further details.

panels show the spatial and angular varieties of GH and IF shifts. In each individual case the polarization modulation basis has been chosen such as to maximize the magnitude of the OAM effect. The overall agreement between experiment and theory is reasonable if we realize that there is no fitting parameter involved; we ascribe the remaining discrepancies to insufficient modal purity of the LG_{10} beam (we are very sensitive to this since we use a quadrant detector).

Fig. 3a shows the spatial GH shift for a polarization basis of diagonal linear polarizations. In this case, the GH shift is absent for $\ell = 0$ but it appears for $\ell = \pm 1$; the sign of the shift reverses when going from $\ell = +1$ to $\ell = -1$. In Fig. 3b we show that the angular IF shift is different for $\ell = 0$ and $\ell = \pm 1$, using again diagonal linear polarizations. No difference occurs for $\ell = +1$ versus $\ell = -1$. Proceeding to Fig. 3c we observe an angular GH shift when using a linear polarization basis (s, p), for both $\ell = 0$ and $\ell = \pm 1$. Both cases show a dispersive resonance at the Brewster angle; for $\ell = 0$ these experimental results have

been reported recently [7] whereas the data for $\ell = \pm 1$ (with opposite sign for $\ell = +1$ and $\ell = -1$) are new. Fig. 3d shows the OAM dependence of the spatial IF shift, observed in a linear polarization basis (s, p) [26]. Here the shift is zero for $\ell = 0$ whereas it shows a dispersive Brewster resonance for $\ell = \pm 1$ (with opposite sign for $\ell = +1$ and $\ell = -1$).

Finally, we have confirmed experimentally that OAM did not affect positional and angular GH and IF shifts in the TIR case (not shown); TIR was realized by flipping the glass prism in Fig. 2.

Conclusions.— We have presented a unified theoretical description of how the Orbital Angular Momentum (OAM) of a light beam affects its kinematic degrees of freedom when the beam is reflected by a dielectric interface. Without OAM the reflection leads to four beam shifts relative to geometrical optics, namely the Goos-Hänchen (GH) and Imbert-Fedorov (IF) shifts, each of which may have a positional and an angular part. We introduce a 4×4 polarization-independent (but ℓ -dependent) coupling matrix that describes the OAM induced mixing of these four shifts when using a quadrant detector. Experimentally, we have confirmed this theory by measuring the four shifts as a function of the angle of incidence, for OAM values $\ell = 0$ and ± 1 . We have observed for the first time the OAM induced positional GH and IF shifts as well as the OAM affected angular GH and IF shifts (see Fig. 3 a,b,c,d). Extension of all this from reflection to transmission (i.e. refraction) is straightforward.

Understanding these effects is important since they generally affect control of OAM beams by mirrors and lenses. The angular shifts are particularly interesting from a metrology point of view, both classically and quantum mechanically, since the corresponding transverse excursion of the beam center grows without limits when the beam propagates; this greatly promotes its detectability [7, 27].

Acknowledgments.— We thank K.Y. Bliokh for stimulating us to measure the OAM-induced GH shift which acted as the seed of this paper. Our work is part of the program of the Foundation for Fundamental Research of Matter (FOM). AA acknowledges support from the Alexander von Humboldt Foundation.

[1] I. Newton, *Opticks*, reprinted by Dover Publications, Inc., New-York (1952); see Query 4 on p. 339.

- [2] F. Goos and H. Hänchen, Ann. Phys. **436**, 333 (1947).
- [3] D. Felbacq, A. Moreau, and R. Smaali, Opt. Lett. **28**, 1633 (2003).
- [4] V. O. de Haan, J. Plomp, T. M. Rekveldt, W. H. Kraan, and A. A. van Well, Phys. Rev. Lett. **104**, 010401 (2010).
- [5] C. Imbert, Phys. Rev. D **5**, 787 (1972).
- [6] F. I. Fedorov, Dokl. Akad. Nauk SSSR **105**, 465 (1955).
- [7] M. Merano, A. Aiello, M. P. van Exter, and J. P. Woerdman, Nat. Photon. **3**, 337 (2009).
- [8] O. Hosten and P. Kwiat, Science **319**, 787 (2008).
- [9] K. Y. Bliokh, A. Niv, V. Kleiner, and E. Hasman, Nature Photonics **2**, 748 (2008).
- [10] A. Aiello and J. P. Woerdman, Opt. Lett. **33**, 1437 (2008).
- [11] A. Mair, A. Vaziri, G. Weihs, and A. Zeilinger, Nature **412**, 313 (2001).
- [12] H. He, M. E. J. Friese, N. R. Heckenberg, and H. Rubinsztein-Dunlop, Phys. Rev. Lett. **75**, 826 (1995).
- [13] V. G. Fedoseyev, Opt. Commun. **193**, 9 (2001).
- [14] K. Y. Bliokh, I. V. Shadrivov, and Y. S. Kivshar, Opt. Lett. **34**, 389 (2009).
- [15] M. Onoda, S. Murakami, and N. Nagaosa, Phys. Rev. E **74**, 066610 (2006).
- [16] H. Okuda and H. Sasada, J. Opt. Soc. A **25**, 881 (2008).
- [17] R. Dasgupta and P. K. Gupta, Opt. Commun. **257**, 91 (2006).
- [18] Y. Fainman and J. Shamir, Appl. Opt. **23**, 3188 (1984).
- [19] A. Aiello, C. Marquardt, and G. Leuchs, Opt. Lett. **34**, 3160 (2009).
- [20] R. F. Gragg, Am. J. Phys. **56**, 1092 (1988).
- [21] L. Mandel and E. Wolf, *Optical coherence and quantum optics* (Cambridge University Press, Cambridge, UK, 1995), 1st ed.
- [22] Here we quantify the GH and IF shifts via the photocurrents I_x/I and I_y/I delivered by the quadrant detector actually used in the experiment, respectively. This furnishes the *median* of the beam intensity distribution. Conversely, in Ref. [14] the same displacements are quantified via the *mean* of the intensity distribution. The difference between these two methods leads to both the trivial prefactor N_ℓ (experimentally eliminated by a detector calibration procedure), and the terms “ 2ℓ ” (instead of “ ℓ ”) in the mixing matrix (7).
- [23] A. Aiello, M. Merano, and J. P. Woerdman, Phys. Rev. A **80**, 061801(R) (2009).
- [24] M. W. Beijersbergen, L. Allen, H. E. L. O. van der Veen, and J. P. Woerdman, Opt. Commun.

- 96**, 123 (1993).
- [25] M. Merano, A. Aiello, G. W. 't Hooft, M. P. van Exter, E. R. Eliel, and J. P. Woerdman, Opt. Expr. **15**, 15928 (2007).
 - [26] In fact, instead of pure p polarization we have used in this case a linear polarization that was 2 degrees out of the plane of incidence. This was done to reduce the very large intensity contrast occurring during $p \leftrightarrow s$ modulation and thus to minimize a parasitic cross-effect on the displacement as synchronously measured by the quadrant detector.
 - [27] N. Treps, N. Grosse, W. P. Bowen, C. Fabre, H.-A. Bachor, and P. K. Lam, Science **301**, 940 (2003).